iVES OENO One vine & wine

DOI: https://doi.org/10.20870/oeno-one.2023.57.4.7598

OPEN ACCESS

ORIGINAL RESEARCH ARTICLE

# Source-sink manipulation does not mitigate the effects of grapevine red blotch virus (GRBV) infection on fruit sugar and flavonoid accumulation in Cabernet-Sauvignon

S. Kaan Kurtural[1,2*], Justin D. Tanner[1], Dimitrios Mainos[1], Runze Yu[1,3], Nazareth Torres[1,4] and Johann Martínez-Luscher[5]

[1] Department of Viticulture and Enology University of California Davis, 1 Shields Avenue, Davis, California 95616, United States
[2] Current address: Kurtural Vineyard Consulting Davis, CA 95618 Unites States
[3] Former post-doctoral scholar. Department of Viticulture and Enology, California State University - Fresno, 2360 Barstow Avenue, Fresno, California 93740, United States
[4] Advanced Fruit and Grape Growing Group, Public University of Navarra, 31006 Pamplona, Spain
[5] Universidad de Navarra-BIOMA, Plant Stress Physiology Group (Associated Unit to CSIC, EEAD, Zaragoza). Irunlarrea 1, E-31008, Pamplona, Navarra, Spain

## ABSTRACT

Grapevine red blotch virus (GRBV) negatively affects the composition of grapevine (*Vitis vinifera* L.) berries by reducing total soluble solids and anthocyanins, leading to economic losses for grape producers. Negative effects of GRBV were suspected to be due to impeded carbon translocation from leaves to fruit which limits sugar and flavonoid accumulation in berries. A two-year trial was conducted to determine whether an increase in source: sink ratio may affect sugar allocation and mitigate the effects of GRBV on Cabernet-Sauvignon plants. Experimental design was factorial (2 by 2) with healthy plants that did not have the virus (GRBV (-)) and plants having GRBV (GRBV (+)) and plants were subjected either untreated (UNT) or cluster thinned down to 10 clusters (CT). Effects of cluster thinning and virus status on leaf and shoot total soluble sugars (TSS), plant water status, leaf gas exchange, berry primary and secondary metabolites, and yield components were measured. The TSS in leaves began to accumulate around *véraison*. In shoot sap, GRBV(-) plants had greater concentration in TSS than GRBV(+) plants. The presence of disease improved plant water status increasing the stem water potential and increasing berry mass. However, juice total soluble solids were consistently lower in GRBV(+) plants despite increasing source: sink ratio by 3× with cluster removal. Likewise, GRBV(+) plants produced berries with lower anthocyanin content at harvest regardless of CT in both years. Our results suggest that GRBV infection severally impeded carbohydrate translocation out of the leaves, and in contrast to healthy plants reducing the number of clusters does not induce a reconcentration of sugars in the remaining clusters.

**KEYWORDS:** anthocyanin, carbohydrate translocation, flavonol, gemini virus, carbohydrate allocation, fruit ripening

*correspondence:
kurtural@gmail.com

*Associate editor:*
Gregory Gambetta

*Received:*
24 May 2023

*Accepted:*
9 November 2023

*Published:*
5 December 2023

## INTRODUCTION

*Grapevine red blotch virus* (GRBV) was identified at the University of California Davis Research Station in Oakville, California in 2008 (Calvi, 2011). The symptoms of GRBV in grapevines were similar to those of grapevine leafroll disease, which is also caused by a virus. However, leafroll virus strains were not detected in plants with GRBV, suggesting GRBV was caused by a different virus (Sudarshana *et al*., 2015). Archival leaf samples of grapevine 'Early Burgundy' collected in Sonoma County, California, in 1940 and stored at the UC Davis herbarium, were found to have GRBV (Al Rwahnih *et al*., 2015). These findings revealed that the newly discovered GRBV was present in vineyards long before the disease was recognized in 2008 and the virus genome characterized in 2011.

The virus's most significant economic effect is diminished fruit quality (Sudarshana *et al*., 2015). Grapevine Red Blotch Disease (GRBD) inhibits ripening, particularly lower sugar content in berry juice and anthocyanin concentrations in berry skin, which negatively affects fruit composition and production value (Martínez-Lüscher *et al*., 2019b). Low sugar and anthocyanin content were suggested to be due to decreased carbon translocation; however, the exact mechanism resulting in those effects was unclear (Bowen *et al*., 2020). The severity of symptoms and their onset have been observed to vary with cultivar, vineyard location, and growing season (Cieniewicz *et al*., 2017).

The suppression of virus inoculum and control of possible vectors in the vineyard are the primary objectives of grapevine virus disease management (Maliogka *et al*., 2015). Despite effective virus elimination strategies employed in the laboratory, there is currently no vineyard treatments to cure grapevines from GRBV, or other viruses, emphasizing the importance of GRBV prevention and management after infection in vineyards. Viruses may be excluded from new vineyards by planting certified virus-free plants (Cieniewicz *et al*., 2017; Golino *et al*., 2017). The possible role of GRBV vectors and reservoirs, and determination of differences across viral isolates and strains were all active areas of research (Bahder *et al*., 2016a) and three-cornered alfalfa leaf hopper has been confirmed to be the vector of GRBV both in cage studies and in vineyard studies (Rumbaugh *et al*., 2021). Studies of the effects of GRBV on the transcriptional and hormonal regulation of grape ripening identified several pathways that were abnormally activated or repressed by GRBV infection during the late stages of fruit ripening and were linked to inadequate carbon translocation into berries and delayed maturity resulting in poor fruit composition (Blanco-Ulate *et al*., 2017; Martínez-Lüscher *et al*., 2019b). When the prevalence of GRBV in a vineyard is > 25 % it is considered significant, because this disease has a direct impact on fruit composition at the farm gate (Ricketts *et al*., 2017; Wallis and Sudarshana, 2016).

In healthy grapevines, the ratio of leaf area to fruit mass is strongly correlated with the amount of carbohydrates accumulated in the juice (Naor *et al*., 2002). As a result, an excessive crop load or smaller than ideal canopy size may delay ripening (Geller and Kurtural, 2013). Conversely, if under cropped, *i.e.* reduced crop mass to leaf area ratio, pruning mass is increased without affecting soluble solids accumulation (Terry and Kurtural, 2011). As a result, yield is sometimes limited in order to balance the source:sink ratio to ensure timely fruit ripening (Terry and Kurtural, 2011). The amount of carbon assimilated by leaves is allocated to many organs of the grapevine, and a fraction of the carbon pool is translocated to the fruit (Martínez-Lüscher and Kurtural, 2021). Martínez-Lüscher and Kurtural (2021) reported several compensatory processes in response to over and under cropping were such as changes in berry ripening, berry size, pruning wood and root reserves and development. Components of yield, such as clusters per vine, berries per cluster, berry mass, and berry soluble solids, are interdependent (Palliotti and Cartechini, 2000), and cluster thinning may advance the beginning of *véraison*, fruit ripening and anthocyanin synthesis depending on timing and intensity of the cluster thinning imposed (Guidoni *et al*., 2008).

Inhibition of berry ripening was reported as the most common response to GRBV infection. Components of yield which include clusters per vine, berry mass, and soluble solids, are susceptible to change together with berry ripening in compensation with each other. Although grapevine source:sink manipulation is the most frequently reported case study, most studies have not considered the impediment of virus infection to this and its subsequent effects on secondary metabolites. The objective of this work was to determine if an increase in source:sink ratio through cluster thinning can alleviate the deleterious effect of GRBV infection on total soluble sugar translocation, plant water status, leaf gas exchange and berry primary and secondary metabolites to understand the utility of cluster thinning as a management strategy for vineyards impacted by GRBV.

## MATERIALS AND METHODS

### 1. Experimental site and experimental design

The experiment was conducted during the consecutive growing seasons of 2020 and 2021 at the University of California Davis, Oakville Experimental Vineyard (38.428 N, 122.409 W; Oakville, CA, USA). The site soil was a Bale-silt loam characterized as deep and gravely clay-loam having a slope less than 2 % (Yu and Kurtural, 2020). The site's climate is considered temperate Mediterranean with a high diurnal temperature range and little to no rain during the growing season (Yu and Kurtural, 2020). The experiment was conducted on *Vitis vinifera* L. cv. 'Cabernet-Sauvignon' Clone FPS08 grafted on 110 Richter (*V. rupestris* Scheele × *V. berlandieri* Planch.) rootstock planted in 2012. The rows were oriented NW-SE and spaced 2 m × 2.4 m (vine × row). Plants were pruned to one-bud spurs and trained to a bilateral cordon on a vertical shoot positioned trellis with a cordon height of 96 cm above the ground level. The plants were shoot thinned to a density of 30 shoots · vine$^{-1}$ at Eichhorn-Lorenz

scale stage 17 (Coombe, 1995). No additional hedging or leaf removal was performed. All other cultural practices, such as vineyard fertilization, pest management and soil management, were carried out according to University of California Cooperative Extension guidelines of the region. Flowering of the plants occurred on 10 May in both 2020 and 2021. Fruit was harvested on 14 September 2020, 127 days after flowering (DAF), and 13 September 2021 (126 DAF).

The vineyard had naturally spread distribution of GRBV. One hundred plants were initially selected based on historical visual assessments and tested for virus status using qPCR on fully expanded leaves collected from shoot bases from plants after *véraison* at the end of each preceding growing seasons (September to October) in 2019, 2020 and 2021 in accordance with previous GRBV studies (Bahder *et al*., 2016). In 2019, plants suspected of having GRBV were selected for testing based on visual leaf symptoms of red blotches while plants suspected to be free of the virus (no leaf symptoms observed) were tested to confirm GRBV(-) status. In subsequent years (2020 and 2021), virus status was reconfirmed by qPCR tests. Briefly, total nucleic acid was extracted from leaf petiole tissue using the MagMax 96 Viral RNA isolation kit with the MagMax Express-96 magnetic particle processor (Thermo Fisher Scientific, USA). No new presence of GRBV were identified in the GRBV(-) plants in the second year of study. Additionally, the samples were screened for the following viruses: grapevine leafroll-associated viruses, including *Grapevine leafroll-associated virus-1* (GLRaV-1), *Grapevine leafroll-associated virus-3* (GLRaV-3), and *Grapevine leafroll-associated virus-4* (GLRaV-4, plus strains 9 and Car) (genus *Ampelovirus*); *Grapevine leafroll-associated virus-2* (GLRaV-2, plus strain 2RG); (genus *Closterovirus*); *Grapevine leafroll-associated virus-7* (GLRaV-7); (genus *Velarivirus*); and *Grapevine rupestris stem-pitting associated virus* (GRSPaV); (genus *Foveavirus*); as described by (Al Rwahnih et al., 2015).

To assess the effects of source-sink manipulation on carbohydrate translocation of GRBV (+) plants, two cropping levels were applied to two virus status levels (GRBV (+) and GRBV(-)) using cluster thinning in both years. At the phenological stage of pea size, about 7 mm berry diameter, clusters were removed to homogenize the number of clusters to approximately 45 clusters per plant within the experiment. The untreated (UNT) plants consisted of 45 clusters per vine. At the same time, cluster thinned (CT) treatment group were manually thinned to 10 clusters per plant. The treatments were arranged in a 2 × 2 factorial experiment in a completely randomized design resulting in four treatment combination groups: UNT GRBV (-), CT GRBV(-), UNT GRBV(+), and CT GRBV(+). Each treatment combination was replicated on four plants for a total of 16 plants in both years (N = 16) where each plant corresponded to one treatment-replicate.

## 2. Weather conditions

The meteorological data for the site was sourced from the California Irrigation Management Information System, CIMIS, station (#77, Oakville, CA, USA) for 2019-2020 and 2020-2021 growing seasons. The station is located at the study site, 160 meters away from the experimental plot. Precipitation and Growing Degree Day accumulation (GDD) for the study site that occurred during the trial is shown in Figure 1. Precipitation was measured from October of the preceding season to October of the current season. GDD measurements began on the 1 April and finished on 30 September of the current season for each year. GDD was calculated for each day with the equation and then summed up for each season starting at budbreak:

CIMIS weather data provided a reference evapotranspiration rate. A crop coefficient was determined based on shade

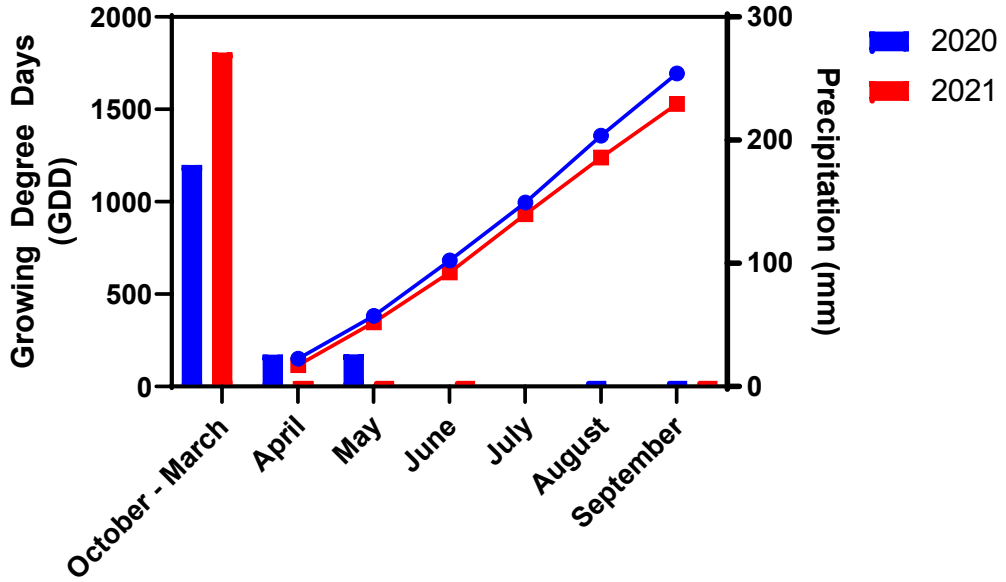


**FIGURE 1.** Growing degree days (lines) and precipitation (bars) at the study site that occurred during the growing seasons of 2019-2020 and 2020-2021. Data was obtained from the CIMIS weather station #77 (Oakville, CA, United States) located at the research site.

cast on the vineyard floor at the study site and used to calculate evapotranspiration by multiplying the reference evapotranspiration and the crop coefficient (Torres *et al*., 2021b). Irrigation was scheduled weekly based on the calculated evapotranspiration to replenish 50 % crop evapotranspiration from fruit set to harvest every year (Torres *et al*., 2021b).

## 3. Plant water status and gas exchange

One fully-expanded and sun-exposed leaf was selected from the main shoot axis on each grapevine and measurements of plant water status. Leaves were covered in Mylar zip-top bags 2 hours before and the assessment of stem water potential ($\Psi_{stem}$) was performed at solar noon with a pressure chamber (Model 615 Pressure Chamber Instrument., PMS Instrument Co., Corvallis, OR, USA). $\Psi_{stem}$ was determined approximately every two weeks from *vérasion* to harvest in both years of study. In 2020, $\Psi_{stem}$ was measured on 23 July (75 DAF), 5 August (87 DAF), 21 August (103 DAF) and 14 September (128 DAF). In 2021, $\Psi_{stem}$ was measured on 27 July (78 DAF), 10 August (93 DAF) and 31 August (114 DAF).

An infrared gas analyzer (CIRAS-3 PP Systems, Amesbury, MA, USA) with a broad leaf chamber (4.5 $cm^2$ window) was used to measure leaf gas exchange of net carbon assimilation ($A_N$) and stomatal conductance ($g_s$). Three measurements from each treatment-replicate were taken around solar noon from an undamaged and mature leaf on the main shoot axis from each data vine for each sampling date. These three measurements were then recorded and averaged to constitute a treatment replicate. Data collection was performed on sunny days with natural sun light (photosynthetically active radiation > 1,500 µmol $m^{-2}$ $s^{-1}$) and the leaf chamber was positioned perpendicularly to sunlight. Chamber conditions were set to 40 % relative humidity, temperature to follow ambient temperature, a reference $CO_2$ concentration of 400 µmol $CO_2$ $mol^{-1}$, and a flow rate of 300 ml $min^{-1}$ into the chamber. During the 2020 growing season, gas exchange was measured on 23 July (75 DAF), 5 August (87 DAF) and 14 September (128 DAF). In 2021, measurements occurred on 27 July (78 DAF), 10 August (93 DAF), and 31 August (114 DAF).

To express the season-long response of $A_N$, and $g_s$, their integrals were calculated by using natural cubic splines for plant water status and gas exchange measurements to assess the cumulative values for these variables over the whole experiment period during each growing season. Then, these cumulative values were normalized as divided by the number of days elapsed between the first measurement date and the last measurement date to make the data comparable to each individual measurement.

## 4. Leaf and shoot sugars determination

During the 2021 growing season leaves were sampled for sugar content on three dates; 14 July (65 DAF, immediate pre- *véraison*), 27 July (78 DAF, *véraison*) and 23 August; (105 DAF, mid- *véraison*) to quantify the concentration of sucrose, fructose, glucose, raffinose, and total soluble sugars as described previously (Torres *et al*., 2021b). Leaf samples from 4-6 mature leaves from each treatment-replicate collected and immediately weighed then oven-dried at 70 °C until weight remained constant. A tissue lyser (MM400, Retsch, Germany) was used to grind the dried leaves into a homogeneous powder. Thirty mg of the resulting powder were extracted in a 75:25 ethanol: water solution at 90 °C for 10 minutes. Immediately after extraction, samples were centrifuged for one minute at 10,000 rpm, and the supernatant was collected and immediately analyzed for the content of sugars. In leaf ethanolic extracts, total and individual sugars were measured, according to Torres *et al.* (2021b). Extracted samples were filtered using PTFE membrane filters (diameter: 13 mm; 0.45 µm; CELLTREAT Scientific Products, Pepperell, MA, USA) and moved into high performance liquid chromatography (HPLC) vials and subjected to reversed-phase HPLC analysis. An Agilent 1100 system along with a diode array detector (DAD) and an Infinity Refractive Index Detector (RID) (Agilent Technologies Inc., Santa Clara, CA, USA) were used. Luna Omega Sugar (150 A 4.6 mm, 3 µm particle size, Phenomenex Inc., Torrance, CA, USA) was used as the reversed-phase column, with a 5 mm guard column. The column compartment was kept at 40 °C, while the RID flow cell was kept at 35 °C. Isocratic elution with acetonitrile: water (75:25, V/V) at a flow rate of 1.0 ml/min and run time of 22 minutes was used in the mobile phase. To determine the retention time for each compound, standard solutions of 10 mg/L D-glucose, D-fructose, D-sucrose, and D-raffinose were injected, and RID was used for their detection. VWR International provided the sugar standards (Radnor, PA, USA). By comparing the peak area and retention time of each sample to standard sample curves, the sugar concentration of each sample was determined.

For the analysis of shoot sugars in phloem sap, a single shoot was collected from each vine on 27 July (78 DAF). A 7 cm stem segment was cut from near the shoot base which had the cluster node located at its center and was used for sap collection. To control for diurnal variation between samples, all shoots were collected at the same time. Sap was extracted placing shoot segments in a 15 ml conical tubes (base downwards) and centrifugating at 4500 rpm for 15 minutes at 4 °C. After centrifuging, extracted sap fluid was collected from the bottom of the tube and weighed. Extracted sap was then diluted by bringing volume up to 1 ml using deionized water and mixed on a vortex mixer. Diluted sap solutions were then filtered using PTFE membrane filters (diameter: 13 mm; 0.45 µm; CELLTREAT Scientific Products, Pepperell, MA, USA) into HPLC vials and immediately subjected to reversed-phase HPLC analysis using the method mentioned above for leaf sugar analysis.

## 5. Berry mass and chemical composition

For the analysis of shoot sugars in phloem sap, a single shoot was collected from each vine on 27 July (78 DAF). A 7 cm stem segment was cut from near the shoot base which had the cluster node located at its center and was used for sap collection. To control for diurnal variation between samples, all shoots were collected at the same time. Sap was extracted placing shoot segments in a 15 ml conical tubes (base

downwards) and centrifugating at 4500 rpm for 15 minutes at 4 °C. After centrifuging, extracted sap fluid was collected from the bottom of the tube and weighed. Extracted sap was then diluted by bringing volume up to 1 ml using deionized water and mixed on a vortex mixer. Diluted sap solutions were then filtered using PTFE membrane filters (diameter: 13 mm; 0.45 µm; CELLTREAT Scientific Products, Pepperell, MA, USA) into HPLC vials and immediately subjected to reversed-phase HPLC analysis using the method mentioned above for leaf sugar analysis.

### 6. Leaf area to fruit ratio and yield components

Leaf area of each treatment-replicate was determined using a smart-phone based program as reported elsewhere (Torres *et al*., 2021a; Yu and Kurtural, 2020). Briefly, Leaf area index (LAI) was measured to characterize grapevine canopy growth and converted into leaf area at *véraison* in each year by a smartphone-based program, VitiCanopy, coupled with an iOS system (Torres *et al*., 2021a). The gap fraction threshold was set to 0.75, the extinction coefficient was set to 0.7, and sub-divisions were 25. A 'selfie-stick' was used to place the device 75 cm underneath the canopy. The device was positioned with the maximum length of the screen being perpendicular to the cordon, and the cordon being at the middle of the screen according to the user's manual (De Bei *et al*., 2016). In each experimental unit, three images were taken to capture half the canopy of each plant and then analyzed by the software. Total leaf areas were calculated based on both LAI values and unit ground area in each experimental unit, and then the leaf area to fruit ratio was calculated. For yield per vine, clusters were removed from plants, counted, and weighed on a top-loading balance when the control treatment (GRBV (-) plants) reached 25°Brix as is a common production practice in the region. The amount of sugars per berry was calculated by multiplying the percent total soluble solids measured at harvest by the berry weight.

### 7. Berry anthocyanin and flavonol content

Immediately at harvest for both years, 20 berries were collected from each vine, berry skins were peeled by hand and placed into 15 mL centrifuge tubes with perforated lids. The berry skins were freeze-dried (Cold Trap 7385020, Labconco, Kansas City, MO, USA) until no change in mass could be detected. A tissue lyser (MM400, Retsch, Germany) was used to grind dried tissues into a fine, homogenous powder to determine the presence and quantity of low molecular weight flavonoid compounds present in the sample. The method described by Martínez-Lüscher *et al.* (2019a) was followed. For each sample, 50 mg of berry skin powder was extracted in methanol: water: 7 M hydrochloric acid (70:29:1, V/V/V), and held at 4 °C overnight. After the extraction, samples were centrifuged for 10 minutes at 4,000 rpm, and supernatant was collected. Extracts were filtered into HPLC vials by using PTFE membrane filters (diameter: 13 mm; 0.45 µm; CELLTREAT Scientific Products, Pepperell, MA, USA), and analyzed on an Agilent 1260 series reversed phase HPLC system (Agilent 1260, Santa Clara, CA, USA) with a DAD. At 25 °C with flow at 0.5 mL per minute, separation was performed on a reversed-phase C18 column LiChrospher ® 100, 250 mm, 4 mm with a 5 µm particle size and a 4 mm guard column of the same material. The mobile phase, which was designed to avoid co-elution of anthocyanins and flavonols (Martínez-Lüscher *et al*., 2019a), consisted of a constant 5.5 % of formic acid and the following gradient (V/V) of acetonitrile in water: 0 minute 8 %, at 25 minutes 12.2 %, at 35 minutes 16.9%, at 70 minutes 35.7 %, 65% between 70 and 75 minutes, and 8 % between 80 and 90 minutes. The peak area of absorbance at 520 nm was used to identify anthocyanins, and absorbance at 365 was used for identification of flavonols. Flavonols and anthocyanins were quantified determining the peak area of the absorbance at 365 nm and 520 nm, respectively, and using quercetin 3-*O*-glucoside and malvidin-3-*O*-glucoside chloride (Extrasynthèse, Genay, France) as quantitative standards.

### 8. Statistical analyses

All data was analyzed using SAS (v. 9.4 SAS Institute, Cary, NC). The same plants were measured in both years during the execution of the experiment. The data was subjected to three-way analysis of variance for a year × virus status × crop level using the PROC GLM procedure of SAS. Whenever the year effect was significant, the analysis was conducted separately for each year. *Post-hoc* analyses were conducted using Duncan's new multiple range test at $p < 0.05$.

## RESULTS

### 1. Stem water potential and leaf gas exchange

Virus status affected $\Psi_{stem}$ integrals in both years of study (Table 1). In 2020, the $\Psi_{stem}$ integrals from GRBV(+) were higher with a mean value of -0.96 MPa compared to GRBV(-) plants at -1.04 MPa indicating GRBV(+) plants had 7.7 % greater $\Psi_{stem}$ than GRBV(-) over the season. In 2021, the $\Psi_{stem}$ integrals from GRBV(+) plants were also significantly higher with a mean value of -1.19 MPa compared to GRBV(-) plants at -1.35 MPa indicating GRBV(+) plants had 11.9 % greater $\Psi_{stem}$ than GRBV(-) over the season. In either year and among years, CT or the interaction of CT and virus status did not have significant effect on plant water status.

Virus status did not affect $A_N$ and $g_s$ integrals in both years of the study (Table 1). The $g_s$ was not affected by CT in 2020. However, in 2021, the CT treatment had 20 % greater $g_s$ than UNT (Table 1). In either year there was no interaction of virus status and CT on leaf gas exchange integrals.

### 2. Leaf and shoot sugars

In 2021, pre- *véraison* (65 DAF) values in leaf total sugar contents or the content of individual sugars were not affected by virus status or CT except glucose (Figure 2). However, at *véraison* (78 DAF) and mid- *véraison* (105 DAF), GRBV affected the total sugar content, sucrose, and fructose content in leaves (Figure 2A, B, C). Leaves from GRBV(+) plants had, on average, 52 % more total sugar content than GRBV(-) (Figure 2A). At mid- *véraison* (105 DAF), the

**TABLE 1.** Effects of Grapevine Red Blotch Virus (GRBV) status and crop level adjustment by cluster thinning on integrals of plant water status (∫ Ψstem), stomatal conductance (∫ $g_s$) and net carbon assimilation (∫ $A_{net}$) measured from verasion to harvest of Cabernet-Sauvignon (clone FPS07) in two successive seasons (2020-2021). Data was collected on 23 July, 2020 (74 DAF), 5 August, 2020 (87 DAF), 14 September, 2020 (127 DAF), 27 July, 2021 (78 DAF), 10 August, 2021 (93 DAF), and 31 August, 2021 (113 DAF) n = 16.

| Treatment | ∫ $\Psi_{stem}$ (MPa) | ∫$g_s$ (mmol $m^{-2}$ $s^{-1}$) | ∫$A_N$ (mmol $m^{-2}$ $s^{-1}$) |
|---|---|---|---|
| *Year 2020* | | | |
| Virus | | | |
| GRBV (-) | - 1.04 b | 173.18 | 12.77 |
| GRBV (+) | - 0.96 a | 184.69 | 13.42 |
| Pr>F | 0.0422 | 0.3359 | 0.4092 |
| Crop level | | | |
| UNT | - 0.99 | 166.78 b | 12.66 |
| CT | - 1.01 | 191.10 a | 13.53 |
| Pr>F | 0.5698 | 0.0458 | 0.2701 |
| Virus × crop level | | | |
| Pr>F | 0.1340 | 0.5137 | 0.3472 |
| *Year 2021* | | | |
| Virus | | | |
| GRBV (-) | - 1.35 b | 76.06 | 9.46 |
| GRBV (+) | - 1.19 a | 90.62 | 9.53 |
| Pr>F | 0.0301 | 0.1554 | 0.9393 |
| Crop level | | | |
| UNT | - 1.29 | 73.97 | 8.48 b |
| CT | - 1.24 | 92.71 | 10.50 a |
| Pr>F | 0.4544 | 0.0698 | 0.0197 |
| Virus × crop level | 0.8535 | 0.6764 | 0.2851 |
| Year | <.0001 | <.0001 | <.0001 |
| Virus × year | 0.3433 | 0.8446 | 0.6081 |
| Virus × crop level | 0.2837 | 0.4412 | 0.8903 |
| Virus × crop level × year | 0.5265 | 0.9741 | 0.3486 |

[z] Statistical significance ($p \leq 0.05$) was determined according to two way ANOVA for virus x crop level factors and three way ANOVA for virus x crop level x year factors. Columns with different letters are significantly different according to Duncan's new multiple range test at $p < 0.05$.

leaves from GRBV(+) had, on average, about 66 % more total NSC than GRBV(-). At this same sampling date, GRBV(+) had 44 % more sucrose and 88 % more fructose than leaves from GRBV(-) plants (Figure 2B, C). The CT treatments did not affect leaf sugar content at any sampling point (Figure 2A). We also did not find an interaction of virus status and CT on leaf sugar contents.

At the onset of *véraison* (74 DAF), NSC concentration in shoot sap of GRBV(-) was statistically greater than GRBV(+), on average, having 66 % more total NSCs (Figure 3A). For fructose, the difference in concentration was even greater with 95 % more in sap fluid from GRBV(-) than GRBV(+) (Figure 3D). Interestingly, no statistical difference in the concentration of sucrose, glucose, or raffinose was measured in sap (Figure 3B, C, E). CT treatments did not affect any of NSCs, nor did we measure an interactive effect of virus status and CT (Figure 3A).

## 3. Berry composition

In both years of study, virus status and CT had a transient effect on berry mass (Figure 4A, E). However, at harvest, the berry mass was not affected by either factor. For virus status, berries from GRBV(+) plants were statistically heavier at individual sampling dates in both years (Figure 4 A, E). In 2020, GRBV(+) berries weighed more at mid-*véraison* (103 DAF) although no difference was observed at other sampling dates in that year (Figure 4A). In 2021, at 58, 85 and 105 DAF berries from GRBV(+) were heavier than GRBV(-) but later sampling at harvest (126 DAF) berry mass was not statistically different (Figure 4E). CT did not affect berry mass in 2020, however in 2021 berries from CT treatment were heavier compared to UNT treatments at 58 DAF and 85 DAF but not different at 105 DAF and 126 DAF.

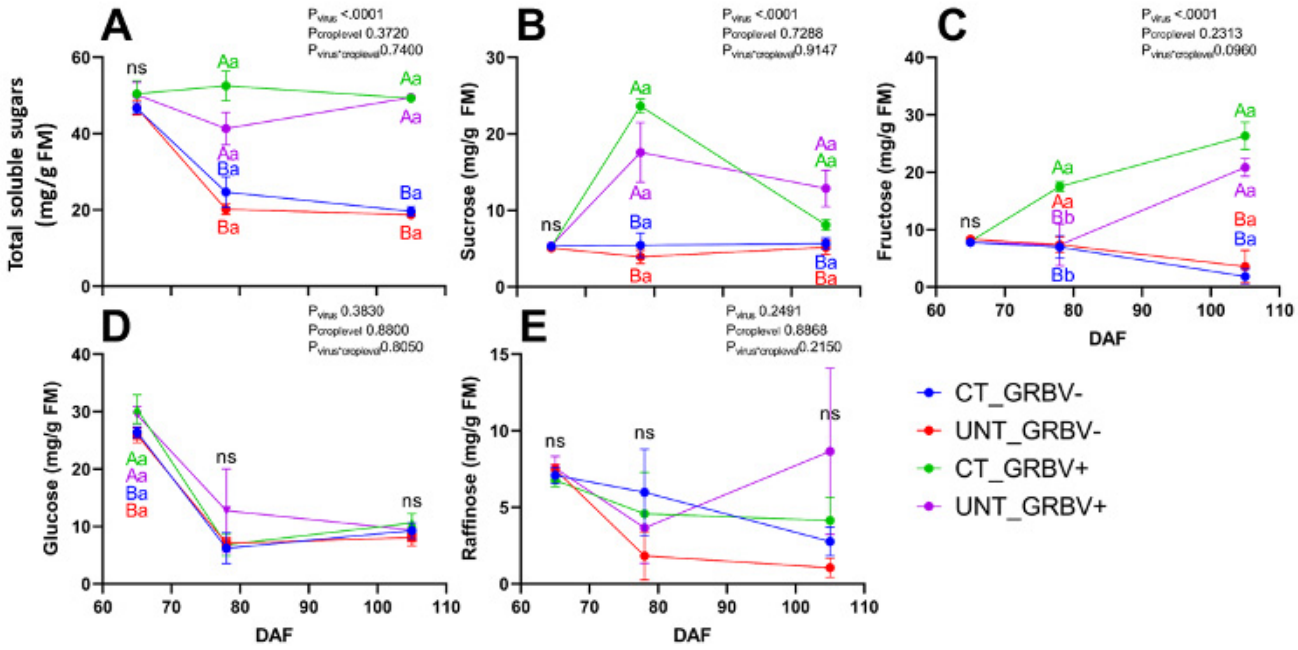


**FIGURE 2.** Effects of Grapevine Red Blotch Virus status and crop level adjustment by cluster thinning on leaf sugar concentration A) total soluble sugars, B) sucrose, C) fructose, D) glucose and E) raffinose of Cabernet-Sauvignon (clone FPS07) during the season of 2021. Leaf samples were collected on 14 July (65 DAF), 27 July (78 DAF) and 23 August (105 DAF). All concentrations are reported in mg/g of fresh mass. Values represent means ± SEM (n = 4). Different letters represent significant differences ($p \leq 0.05$) according to two-way ANOVA followed by Duncans's new multiple range test. Difference in capital letters represent significant differences due to virus effect while lower case letters indicate difference due to crop level effect.

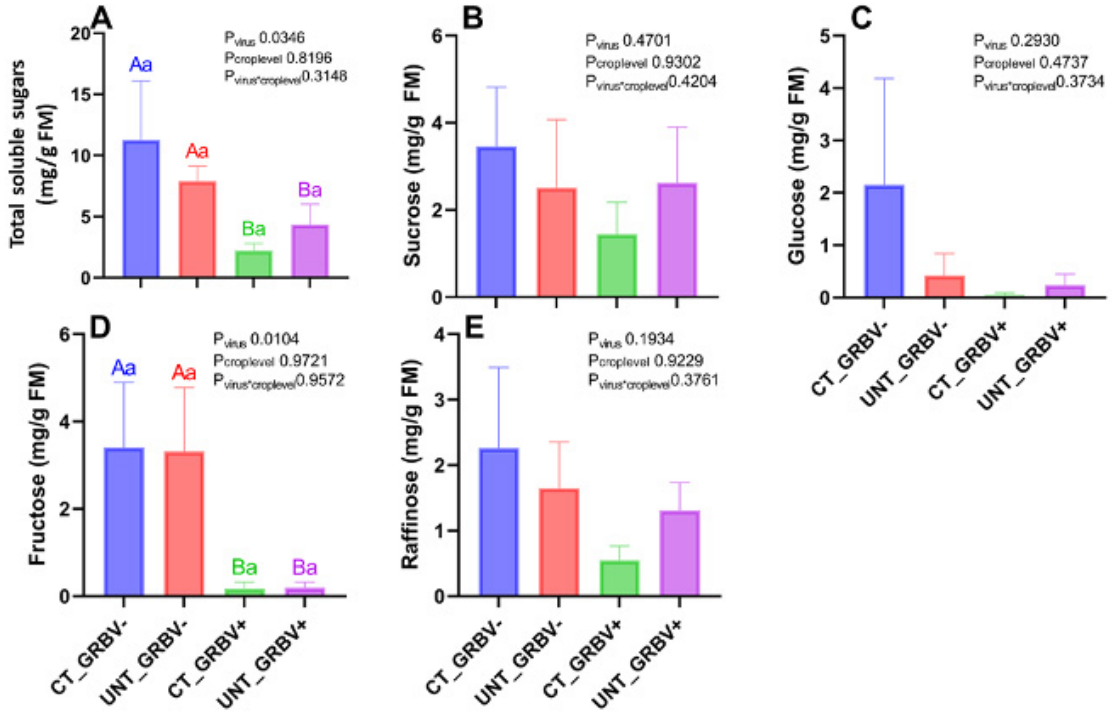


**FIGURE 3.** Effects of Grapevine Red Blotch Virus status and crop level adjustment by cluster thinning on sap sugar concentration at the onset of *véraison* A) total soluble sugars, B) sucrose, C) fructose, D) glucose and E) raffinose of Cabernet-Sauvignon (clone FPS07) during the season of 2021. Sap samples were collected from 7 cm stems segments on 23 July (74 DAF). All concentrations are reported in mg/g of fresh mass. Values represent means ± SEM (n = 4). Different letters represent significant differences ($p \leq 0.05$) according to two-way ANOVA followed by Duncans's new multiple range test. Difference in capital letters represent significant differences due to virus effect while lower case letters indicate difference due to crop level effect.

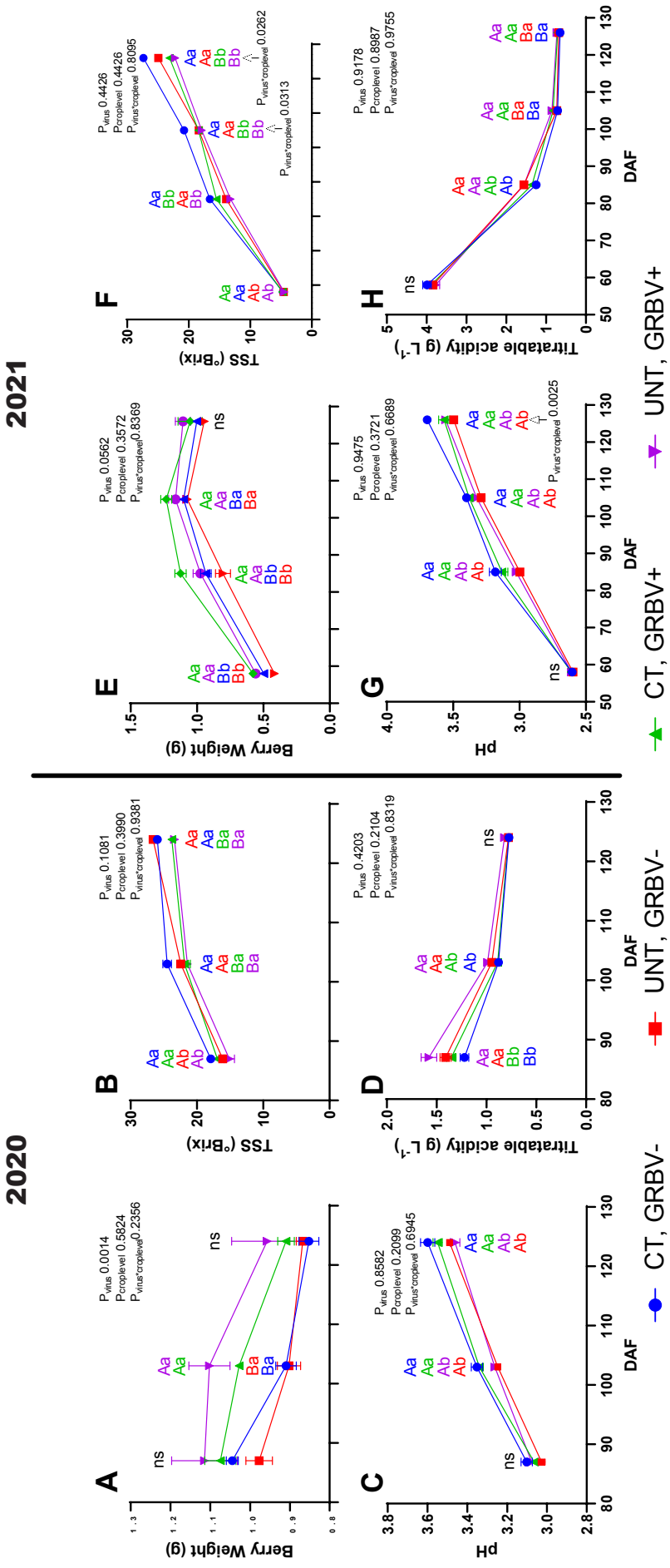


**FIGURE 4.** Effects of Grapevine Red Blotch Virus status and crop level adjustment by cluster thinning on Cabernet-Sauvignon (clone FPS07) fruit components of primary metabolites A,E) berry weight, B,F) total soluble solids (°Brix), C,G) pH, D,H) titratable acidity. Left panels show values from 2020 season A-D), while right panels show 2021 results E-H). In 2020, berry samples were collected on 5 August (87 DAF), 21 August (103 DAF) and 11 September (124 DAF). In 2021, samples were collected on 7 July (58 DAF), 3 August (85 DAF), 23 August (105 DAF) and 13 September (126 DAF). Values shown represent means ± SEM (n = 4). Different letters represent significant differences ($p \leq 0.05$) according to two-way ANOVA followed by Duncans's new multiple range test. Difference in capital letters represent significant differences due to virus effect while lower case letters indicate difference due to crop level effect.

**TABLE 2.** Effects of GRBV status and crop level adjustment by cluster thinning on components of yield of Cabernet-Sauvignon (clone FPS07) grafted on 110R over two successive growing seasons (2020-2021). Harvest was conducted on 14 September, 2020 (127 DAF) and 13 September, 2021 (126 DAF).

| Treatment | Yield (kg·vine$^{-1}$) | Cluster number | Cluster weight (g) | Leaf area: fruit ($m^2.kg^{-1}$) | Sugar/berry (mg berry$^{-1}$) |
|---|---|---|---|---|---|
| *Year 2020* | | | | | |
| Virus | | | | | |
| GRBV (-) | 2.61 | 25 | 110.12 | 4.21 | 0.260 a |
| GRBV (+) | 3.83 | 28 | 131.87 | 2.95 | 0.231 b |
| Pr>F | 0.1082 | 0.3400 | 0.0949 | 0.1188 | 0.0001 |
| Crop level | | | | | |
| UNT | 5.07 | 43 | 116.17 | 1.59 b | 0.25 |
| CT | 1.37 | 11 | 125.82 | 5.98 a | 0.26 |
| Pr>F | 0.0002 | 0.0001 | 0.4368 | 0.0001 | 0.9988 |
| Virus × crop level | | | | | |
| *Year 2021* | | | | | |
| Virus | | | | | |
| GRBV (-) | 3.72 | 27 | 143.27 | 3.23 | 0.271 a |
| GRBV (+) | 4.60 | 30 | 151.35 | 3.42 | 0.243 b |
| Pr>F | 0.1925 | 0.0750 | 0.6750 | 0.8098 | 0.0001 |
| Crop level | | | | | |
| UNT | 6.88 | 48 | 144.34 | 1.15 b | 0.26 |
| CT | 1.44 | 10 | 150.28 | 5.50 a | 0.27 |
| Pr>F | <.0001 | <.0001 | 0.7573 | 0.0002 | 0.8843 |
| Virus × crop level | 0.1767 | 0.1067 | 0.4058 | 0.6128 | 0.7771 |
| Year | 0.058 | 0.2759 | 0.0267 | 0.2176 | 0.0871 |
| Virus × year | 0.7316 | 0.8748 | 0.5453 | 0.5512 | 0.7368 |
| Virus × crop level | 0.0687 | 0.3488 | 0.2165 | 0.2289 | 0.2217 |
| Virus × crop level × year | 0.3408 | 0.2721 | 0.9319 | 0.8819 | 0.9912 |

[z] Statistical significance ($p \leq 0.05$) was determined according to two way ANOVA for virus x crop level factors and three way ANOVA for virus x crop level x year factors. Columns with different letters are significantly different according to Duncan's new multiple range test at $p < 0.05$.

Virus status significantly affected Brix in both years (Figure 4 B, F). In 2020, Brix at 87 DAF was not affected statistically by GRBV. However, by mid-*véraison* (103 DAF) and at harvest (124 DAF) GRBV(+) berries had a significantly lower Brix than from GRBV(-) (Figure 4B). At harvest GRBV(+) plants had 10 % less Brix than GRBV(-). In 2021, differences in Brix were affected by virus status and CT treatments as the season progressed from *véraison* (85 DAF) to harvest (126 DAF) as well (Figure 4F). At pre- *véraison* (58 DAF), there was no effect of GRBV on Brix. However, the CT increased Brix at pre-*véraison*. By mid-*véraison* (105 DAF), an interaction of virus status and CT was evident on Brix, and this interaction continued to harvest (126 DAF) (Figure 4F). At harvest in 2021, GRBV(+) plants produced berries that had 13 % less Brix than berries from GRBV(-). GRBV(+) plants that received CT had 23.15 % Brix and did not attain the same Brix levels seen in GRBV(-) plants under either CT treatment. GRBV(-) plants that were CT treated had a mean of 27.40 %Brix while GRBV(-) UNT plants reached 24.95 %Brix. GRBV(+) plants in which no cluster thinning had occurred (UNT) had the lowest mean value at 22.23 %Brix. Although CT increased Brix, the removal of approximately 2/3 of the sinks was unable to compensate for the reduction in Brix caused by the GRBV.

Over two seasons of study, virus status did not influence juice pH (Figure 4C, G). CT treatment, however, did affect pH at several sampling dates in the study, where CT treatment increased pH compared to UNT treatment groups. This effect was statistically different on two of three sampling dates in 2020 (103 DAF and 124 DAF) and one of the four sampling dates in 2021 (85 DAF). Interestingly, virus status and CT factor interactions were not observed in either year in pH or TA. In 2020, CT effects on juice pH was observed at mid-*véraison* (103 DAF) and persisted to harvest (124 DAF) (Figure 4C). For juice TA in 2020, both treatment factors were different at 87 DAF but not at mid-*véraison* (103 DAF) or at harvest (124 DAF) (Figure 4D). At mid- *véraison* (103 DAF) only CT factors influenced juice TA, and by harvest

(124 DAF) no differences were measured between treatments. In 2021, virus status influenced juice TA from mid-*véraison* (105 DAF) until harvest (126 DAF) (Figure 4H). CT had a transient effect on TA, which was only observed at the start of *véraison* (85 DAF) in 2021. Juice pH was influenced by CT in 2021 at the start of *véraison* (85 DAF), through mid-*véraison* (105 DAF) and continuing into harvest (126 DAF). At harvest (126 DAF), a statistical interaction between CT and virus status was observed with CT treatments having a higher juice pH compared to UNT treatments.

### 4. Yield components and leaf area to fruit ratio

GRBV(+) plants produced yields that were slightly higher than GRBV(-) in both years of study but were not statistically different for individual years (Table 2). In both years, yield was directly affected by CT with UNT groups having significantly more yield compared to CT as a direct result of the CT treatment; removal of clusters in CT treatment groups reduced yield. Reduction in yield due to CT was considerable in both years where, on average, 75 % of the crop was removed.

The leaf area to fruit ratio (LA:FR) was not affected by virus status in either year. However, CT affected LA:FR similarly in both years. The LA:FR of CT was ~3× in each year when compared to UNT (Table 2).

The sugars per berry at the harvest were influenced by the virus status of the grapevines in both years (Table 2). The GRBV(-) plants had accumulated substantially more sugars per berry despite having lower berry mass in both years of the trial when compared to GRBV(+) plants. The CT treatments did not affect the amount of sugars per berry in either year.

### 5. Berry flavonoids

In 2020, anthocyanin content was not affected by virus status or CT treatments (Figure 5). However, in 2021, GRBV reduced total anthocyanins, 3'4' hydroxylated anthocyanins, 3'4'5' hydroxylated anthocyanins, and total methylated anthocyanins (Figure 5A, B, C, D). In 2021, at harvest (126 DAF) berries from GRBV(-) had on average 43% more total anthocyanins, 47% more 3'4' hydroxylated anthocyanins, 43 % more 3'4'5' hydroxylated anthocyanins, and 38 % more methylated anthocyanins than GRBV(+). As for the the flavonols, hydroxylated proportions of the mono-substituted flavonol kaempferol-3-glucoside monitored were not affected in either year by virus status or CT (Figure 6).

## DISCUSSION

### 1. Stem and leaf water potential

Stomatal conductance and $Y_{stem}$ are both regarded as reliable indicators of water status (Torres, Yu, et al., 2021). GRBV(+) plants had higher plant water status corroborating previous works (Copp and Levin, 2021; Martínez-Lüscher *et al*., 2019b). Leaf gas exchange integrals measured indicated that despite having a higher plant water status in GRBV(+) plants in both years, this was not coupled to increases in $g_s$, or $A_N$ integrals in either year. Cluster thinning treatments did not affect $Y_{stem}$ in either year but increased $g_s$ integrals in 2020 and increased $A_N$ integrals in 2021. In previous work in similar climate, $A_N$ integral values were not significantly different among virus status in either year suggesting GRBV(+) status did not reduce photosynthesis or result in a diminished pool of photoassimilates compared to GRBV(-) under the same field conditions (REF missing). Although some studies have reported transient reductions in $g_s$ and $A_N$ in GRBV infected vines, overall, GRBV does not constitute a clear impediment for carbon fixation and stomatal behaviour (Copp and Levin, 2021; Pereira *et al*., 2021; Reynard *et al*., 2018).

### 2. Leaf and shoot sugars

The increase in leaf sugar content in GRBV(+) plants measured in this study corroborated results reported by others (Swamy *et al*., 2021; Wallis and Sudarshana, 2016). Wallis and Sudarshana (2016) reported increased mean carbohydrate values in GRBV(+) leaves from two sampling dates in two different winegrape cultivars; 'Cabernet Franc had increased fructose and glucose levels while 'Cabernet-Sauvignon' had increased glucose compared to GRBV(-) plants. Swamy *et al*. (2021) also reported greater NSC content in leaves of GRBV(+) plants as well as a higher leaf starch content, providing further evidence of GRBV affecting non-structural carbohydrate translocation. Cluster thinning did not have a lasting effect on decreasing sugar accumulation in leaves of GRBV(+) plants (only transiently decreased fructose at DAF 78 in 2021) suggesting that changing sink strength does not change the flow of NSC out of leaf tissues. If NSC translocation were increased by CT in GRBV(+) plants it could be expected that less sugar would accumulate in leaves similar to the levels observed in GRBV(-) plants.

The paradoxical relationship between $g_s$ and $\Psi_{stem}$ observed for GRBV(+) plants may relate to the accumulation of carbohydrates within the leaves caused by transient restricted sugar translocation resulting in feedback inhibition resulting in stomatal closure (Copp *et al*., 2022; Martínez-Lüscher *et al.*, 2019b). It has been reported that when the rate of sucrose production exceeds the rate of export via the phloem, surplus sugars are carried by the transpiration stream toward the stomata, promoting stomatal closure (Kelly *et al*., 2013). The divergence of sugars to stomatal guard cells may be responsible for the improved plant water status observed in GRBV(+) plants in this study.

Contrarily to leaf carbohydrates, GRBV(+) plants had significantly lower content of sugars in phloem sap at sampling 78 DAF. It i expected that reduction in carbohydrate sinks imposed by CT would result in greater availability of carbohydrates in sap moving to remaining fruit; however, CT had no significant effect on phloem sap sugar contents. These results further support the hypothesis that GRBV results in impaired sugar translocation into fruit (Martínez-Luscher *et al*., 2019), severely impacting source: sink relationship. The CT treatment did not affect sugar contents of leaves from GRBV(+) plants; and thus, the reduction carbohydrate translocation from GRBV infected leaves is not modulated buy number of sinks the plant has. This suggested that GRBV infection reduced sugar translocation to a very specific

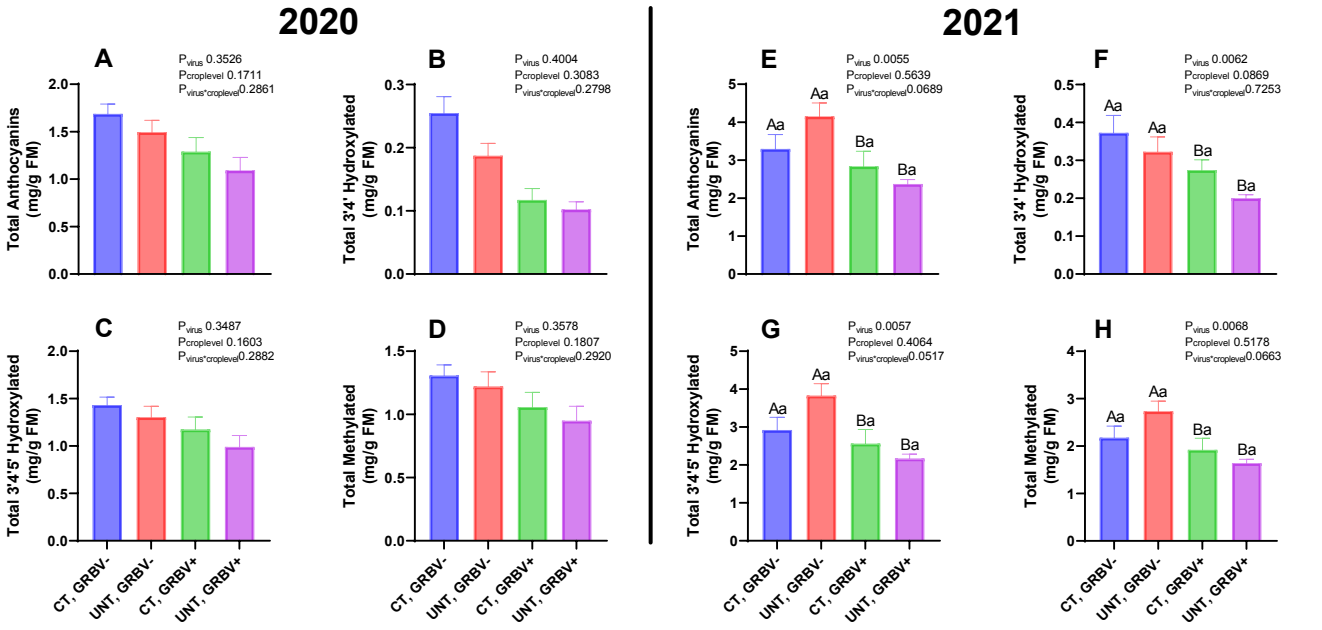


**FIGURE 5.** Effects of Grapevine Red Blotch Virus status and crop level adjustment by cluster thinning on Cabernet-Sauvignon (clone FPS07) fruit secondary metabolites anthocyanins in berry skins A,E) total anthocyanins, B,F) total 3'4' hydroxylated, C,G) 3'4'5 hydroxylated, D,H) total methylated. Left panels show values from 2020 season A-D), while right panels show 2021 E-H). In 2020, berries were collected on 11 September (124 DAF) and on 13 September (126 DAF) in 2021. Values represent means ± SEM (n = 4). Different letters represent significant differences ($p \leq 0.05$) according to two-way ANOVA followed by Duncans's new multiple range test. Difference in capital letters represent significant differences due to virus effect while lower case letters indicate difference due to crop level effect.

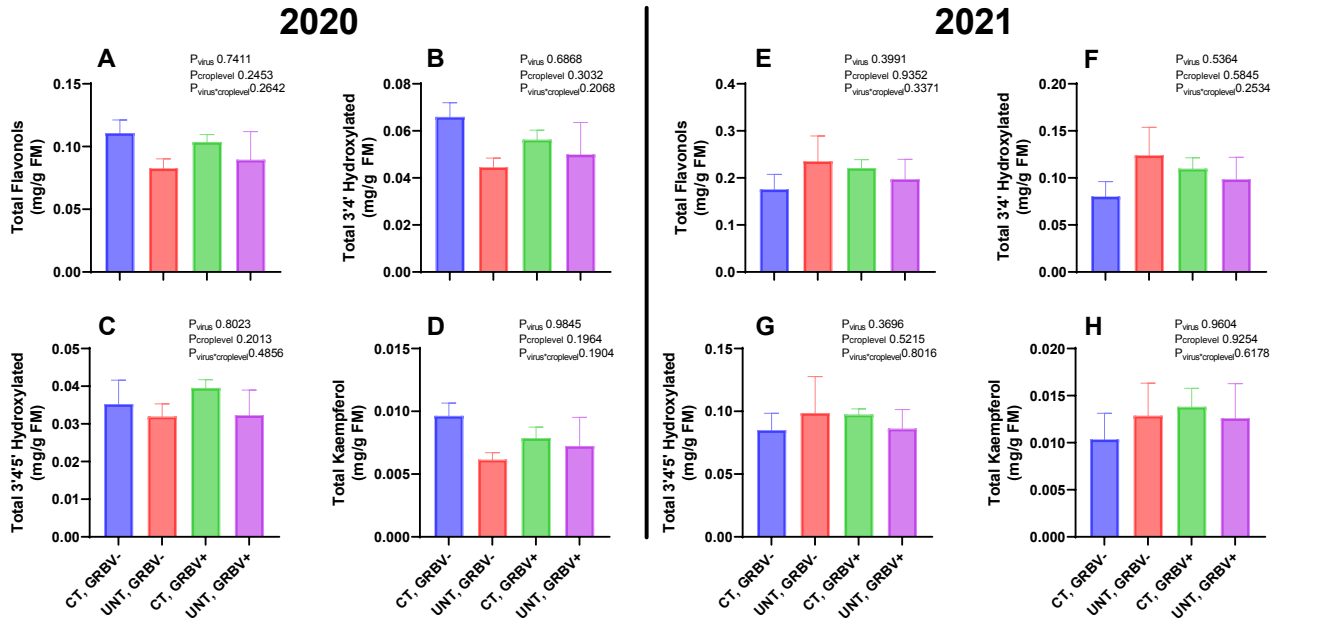


**FIGURE 6.** Effects of Grapevine Red Blotch Virus status and crop level adjustment by cluster thinning on Cabernet-Sauvignon (clone FPS07) fruit secondary metabolites flavonols in berry skins A,E) total flavonols, B,F) total 3'4' hydroxylated, C,G) 3'4'5 hydroxylated, D,H) total kaempferol. Left panels show values from 2020 season A-D), while right panels show 2021 E-H). In 2020, berries were collected on 11 September (124 DAF) and on 13 September (126 DAF) in 2021. Values represent means ±SEM (n = 4). Different letters represent significant differences ($p \leq 0.05$) according to two-way ANOVA followed by Duncan's new multiple range test.

extent, and this limitation cannot be modulated by a higher sugar availability as it would be expected in healthy plants with increased source: sink ratios.

## 3. Berry composition

Results of increased berry weights from GRBV(+) plants reported in this study agree with previous reports (Bowen *et al*., 2020; Copp *et al*., 2022; Pereira *et al*., 2021). Larger berries from GRBV(+) grapes could be attributed to a poor fruit set (Geller and Kurtural, 2013), which decreased competition among berries within a cluster making more room for development and causing reallocation of water. The increased berry weight in GRBV(+) plants in this study were most certainly related to the better water status of these plants. Better water status is known to increase berry size (Matthews and Anderson, 1989), which may dilute berry solute contents and contribute to explain the lower sugar content in GRBV(+) plants.

Sugar accumulation is a critical aspect of the berry ripening process. During the ripening phase of grape berry development sucrose transferred via phloem from leaves is converted to its two monosaccharide constituents, fructose, and glucose, by invertase enzymes which continue to import hexose during this phase causing accumulation in berry vacuoles (Davies and Robinson, 1996). A reduction in berry sugar accumulation from GRBV(+) plants compared to GRBV(-) plants observed in this study were similar to previous reports suggesting that GRBV resulted in less accumulation of sugars in grape berries (Bowen *et al*., 2020; Lee *et al*., 2021; Poojari *et al*., 2013). There was no difference in season-long leaf carbon assimilation rates regarding virus status, implying that the initial pool of carbohydrates was similar between GRBV(-) and GRBV(+) plants. The reduction in Brix from berries or amount of sugar per berry at harvest of GRBV(+) plants may be partially explained by increased levels of foliar sugars measured in GRBV(+) plants. This sugar export deficit may result in physiological stress from the impediment of carbohydrate translocation out of the leaf through the phloem sap ultimately reducing sugar accumulation potential. The present study confirms what postulated in (Martínez-Lüscher *et al*., 2019) that the typical process of sugar transfer from leaves to berries may be altered due to a phloem disfunction by GRBV, resulting in increased sugar content in leaves and decreased sugar accumulation in berries.

Results of CT effects on berry sugar accumulation from this study agreed with previous reports which found inconsistent effect in sugar accumulation in GRBV(+) plants (Copp *et al*., 2022). In results from 2021 presented in this study, CT treatment was shown to improve BRIX in GRBV(+) plants but the increase was significantly less than UNT GRBV(-) control. This result suggested CT adjustments cannot overcome the negative impact of reduced BRIX from GRBV(+) plants. Even with a drastic 78 % reduction in CT imposed by CT treatment in this trial, fruit composition was still diminished by GRBV(+) compared to GRBV(-) plants. Coupled with leaf and phloem sap sugar concentration data presented in this study, regardless of CT, GRBV disrupted the translocation from source to sink when compared to GRBV(-) plants.

Virus status was not observed to significantly affect berry juice pH at any date in either year of the study while TA increased due to GRBV at different times in both years. Previous studies reported berry juice of GRBV(+) plants having higher pH and TA (Bowen *et al*., 2020) while others observed TA was higher but the pH was lower (Rumbaugh *et al*., 2021). Results from this two-year study agree with the results of Martínez-Lüscher *et al*. (2019) that reported GRBV(+) berries having higher TA but no significant difference in pH compared to GRBV(-) controls. This result is remarkable considering that normally an increase in berry juice TA would be accompanied by a decrease in juice pH (Keller, 2020).

## 4. Yield components and leaf area to fruit

Virus status did not have an impact on yield in either 2020 or 2021, in agreement with other reports (Lee *et al*., 2021). However, many previous reports observed lower yield from GRBV(+) plants (Bowen *et al*., 2020; Buchs *et al*., 2018; Cieniewicz *et al*., 2017; Poojari *et al*., 2013). Cluster weights were not affected by GRBV, in agreement with previous reports (Lee et al., 2021). The LA:FR values achieved within the context of this trial corroborated previous works, crop level manipulation by CT inflated the LA:FR (Geller and Kurtural, 2013; Martínez-Lüscher and Kurtural, 2021). Based on the plant density and the trellis used, the LA:FR would be optimized at 1.2-1.5 $m^2.kg^{-1}$ (Martínez-Lüscher and Kurtural, 2021; Terry and Kurtural, 2011). The GRBV (-/+) plants that received CT treatment resulted in 3× this range, an indication of too much leaf area for the amount of fruit carried. Conversely, the UNT treatment had appropriate LA:FR ratio that was adequate to achieve ripeness at the correct speed (Naor *et al*., 2002).

## 5. Berry flavonoids

Sucrose stimulus in berries was identified as both a trigger and substrate for anthocyanin biosynthesis in ripening grape berries (Dai *et al*., 2014). As a result, a decrease in translocation of carbohydrates to GRBV(+) berries from the leaf could be the direct cause of decreased anthocyanins production. Discrepancy on anthocyanin content between years may relate to differences in mean daily temperature, as 2020 had less diurnal variation of temperatures, which may have caused anthocyanin degradation in 2020 (Torres *et al*., 2020). And this might also have resulted in no significant difference between treatments at harvest despite skin anthocyanin means from GRBV(+) plants being lower. A reduction in berry skin anthocyanin concentration in 2021 agreed with previous work which found GRBV decreased anthocyanin biosynthesis in berry skins (Martínez-Lüscher, Brillante, et al., 2019). Data of anthocyanin concentration in berry skins when considered together with results of B from berry juice revealed GRBV affects primary metabolism and as a result cascaded into reduction of capacity for anthocyanins biosynthesis. In this study, CT treatments did not have a significant effect on total, total 3'4'5' hydroxylated, or total methylated anthocyanin concentration, which corroborated

with the results from (Copp *et al*., 2022; Copp and Levin, 2021) that also reported such a practice did not significantly improve anthocyanin concentration.

Red and black skinned grape berries present a wide range of anthocyanin and flavonol profiles. Grapevines used in full-bodied wine production have a high 3' and 5' substituted profile that are rich in anthocyanin and flavonols with hydroxyl or methyl groups of the B-ring (Torres *et al*., 2021). Flavonols in grape berry are modulated by exposure to solar radiation (Torres *et al*., 2020). In previous works, abundance of kaempferol (Martínez-Lüscher *et al*., 2019) was identified as an indicator of grapevine canopy porosity. Since the leaf area was unaltered during the experiment, it would be plausible that flavonol concentration and proportion of flavonols and therefore kaempferol abundance would be unchanged. This was also revealed in our results where no change in flavonol concentration or their hydroxylation ratio at harvest was affected by virus status or CT. This lack of response from the flavonol profile indicated that GRBV infection does not alter canopy microclimate adversely.

Our results provided evidence that GRBV significantly inhibited translocation of photoassimilates from the source organs as the leaves, through sap flow in shoots to the sink organs as the fruits. By quantifying sugar concentrations in leaves, phloem sap, and fruits, a more complete perspective on the effect of GRBV on grapevine physiology and berry composition in relation to a proposed alleviation strategy, CT, was revealed. Additionally, when considering anthocyanin biosynthesis in GRBV(+) plants, an impediment of carbohydrate transport from source to sink affected secondary metabolites, further reducing anthocyanin concentration in berries. Results from this two-year study provided evidence that CT did not reallocate sugars to fruit and it would not be a successful strategy to mitigate effects of GRBV.

## ACKNOWLEDGEMENTS

The authors acknowledge funding provided by the USDA-NIFA 2019-51181-30020 for the execution of the project

## REFERENCES

Al Rwahnih, M., Rowhani, A., & Golino, D. (2015). First Report of Grapevine Red Blotch-Associated Virus in Archival Grapevine Material from Sonoma County, California. *Plant Dis*, *99*(895). https://doi.org/10.1094/PDIS-12-14-1252-PDN

Bahder, B. W., Zalom, F. G., Jayanth, M., & Sudarshana, M. R. (2016). Phylogeny of Geminivirus Coat Protein Sequences and Digital PCR Aid in Identifying Spissistilus festinus as a Vector of Grapevine Red Blotch-Associated Virus. *Phytopathology*, *106*, 1223–1230. https://doi.org/10.1094/PHYTO-03-16-0125-FI

Blanco-Ulate, B., Hopfer, H., Figueroa-Balderas, R., Ye, Z., Rivero, R. M., Albacete, A., Pérez-Alfocea, F., Koyama, R., Anderson, M. M., Smith, R. J., Ebeler, S. E., & Cantu, D. (2017). Red blotch Disease Alters Grape Berry Development and Metabolism by Interfering with the Transcriptional and Hormonal Regulation of Ripening. *J. Exp. Bot*, *68*, 1225–1238. https://doi.org/10.1093/jxb/erw506

Bowen, P., Bogdanoff, C., Poojari, S., Usher, K., Lowery, T., & Úrbez-Torres, J. R. (2020). Effects of Grapevine Red Blotch Disease on Cabernet franc Vine Physiology, Bud Hardiness, and Fruit and Wine Quality. *Amer. J. Enol. Viticult*, *71*, 308–318. https://doi.org/10.5344/ajev.2020.20011

Buchs, N., Braga-Lagache, S., Uldry, A.-C., Brodard, J., Debonneville, C., Reynard, J.-S., & Heller, M. (2018). Absolute Quantification of Grapevine Red Blotch Virus in Grapevine Leaf and Petiole Tissues by Proteomics. *Front. Plant Sci*, *9*(1735). https://doi.org/10.3389/fpls.2018.01735

Calvi, B. L. (2011). *Effects Of Red-leaf Disease on Cabernet-Sauvignon at the Oakville Experimental Vineyard and Mitigation by Harvest Delay and Crop Adjustment* [MS Thesis,]. Univ. CA.

Cieniewicz, E., Perry, K., & Fuchs, M. (2017). *Grapevine Red Blotch: Molecular Biology of the Virus and Management of the Disease* (B. Meng, G. P. Martelli, D. A. Golino, & M. Fuchs, Eds.). Molecular Biology, Diagnostics and Management. Springer. https://doi.org/10.1007/978-3-319-57706-7_14

Copp, C. R., Kc, A. N., & Levin, A. D. (2022). Cluster Thinning Does Not Improve Fruit Composition in Grapevine Red Blotch Virus-infected *Vitis vinifera*. *Am J Enol Vitic*, *73*, 56–66. https://doi.org/10.5344/ajev.2021.21016

Copp, C. R., & Levin, A. D. (2021). Irrigation Improves Vine Physiology and Fruit Composition in Grapevine Red Blotch Virus-Infected *Vitis vinifera* L. *Am J Enol Vitic*, *72*, 307–317. https://doi.org/10.5344/ajev.2021.21007

Dai, Z. W., Meddar, M., Renaud, C., Merlin, I., Hilbert, G., Delrot, S., & Gomès, E. (2014). Long-Term In Vitro Culture of Grape Berries and its Application to Assess the Effects of Sugar Supply on Anthocyanin Accumulation. *J. Exp*, *65*, 4665–4677. https://doi.org/10.1093/jxb/ert489

Davies, C., & Robinson, S. P. (1996). Sugar Accumulation in Grape Berries (Cloning of Two Putative Vacuolar Invertase cDNAs and Their Expression in Grapevine Tissues. *Plant Physiology*, *111*, 275–283. https://doi.org/10.1104/pp.111.1.275

Geller, J. P., & Kurtural, S. K. (2013). Mechanical Canopy and Crop-Load Management of Pinot Gris in a Warm Climate. *Amer. J. Enol. Viticult*, *64*, 65–73. https://doi.org/10.5344/ajev.2012.12045

Golino, D. A., Fuchs, M., Sim, S., Farrar, K., & Martelli, G. P. (2017). *Improvement of Grapevine Planting Stock Through Sanitary Selection and Pathogen Elimination* (B. Meng, G. P. Martelli, D. A. Golino, & M. Fuchs, Eds.). Molecular Biology, Diagnostics and Management. Springer International Publishing. https://doi.org/10.1007/978-3-319-57706-7_27

Guidoni, S., Ferrandino, A., & Novello, V. (2008). Effects of Seasonal and Agronomical Practices on Skin Anthocyanin Profile of Nebbiolo Grapes. *Amer. J. Enol. Viticult*, *59*, 22–29. https://doi.org/10.5344/ajev.2008.59.1.22

Keller, M. (2020). *The Science of Grapevines*. Academic Press.

Kelly, G., Moshelion, M., David-Schwartz, R., Halperin, O., Wallach, R., Attia, Z., Belausov, E., & Granot, D. (2013). Hexokinase Mediates Stomatal Closure. *Plant J*, *75*, 977–988. https://doi.org/10.1111/tpj.12258

Lee, J., Rennaker, C. D., Thompson, B. D., & Karasev, A. V. (2021). Influence of Grapevine Red Blotch Virus (GRBV) on Idaho 'Syrah' Grape Composition. *Sci. Hortic*, *282*(110055). https://doi.org/10.1016/j.scienta.2021.110055

Maliogka, V. I., Martelli, G. P., Fuchs, M., & Katis, N. I. (2015). *Chapter Six—Control of Viruses Infecting Grapevine* (G. Loebenstein & N. I. Katis, Eds.). Adv. Virus Res., Contr. Plant Virus Dis. Academic Press. https://doi.org/10.1016/bs.aivir.2014.11.002

Martínez-Lüscher, J., Brillante, L., & Kurtural, S. K. (2019). Flavonol Profile Is a Reliable Indicator to Assess Canopy Architecture and the Exposure of Red Wine Grapes to Solar Radiation. *Front. Plant Sci*, *10*(10). https://doi.org/10.3389/fpls.2019.00010

Martínez-Lüscher, J., & Kurtural, S. K. (2021). Same Season and Carry-Over Effects of Source-Sink Adjustments on Grapevine Yields and Non-structural Carbohydrates. *Front. Plant Sci*, *12*. https://doi.org/10.3389/fpls.2021.695319

Martínez-Lüscher, J., Plank, C. M., Brillante, L., Cooper, M. L., Smith, R. J., Al-Rwahnih, M., Yu, R., Oberholster, A., Girardello, R., & Kurtural, S. K. (2019). Grapevine Red Blotch Virus May Reduce Carbon Translocation Leading to Impaired Grape Berry Ripening. *J. Agric. Food Chem*, *67*, 2437–2448. https://doi.org/10.1021/acs.jafc.8b05555

Matthews, M. A., & Anderson, M. M. (1989). Reproductive Development in Grape (*Vitis vinifera* L.): Responses to Seasonal Water Deficits. *Amer. J. Enol. Viticult*, *40*, 52–60. https://doi.org/10.5344/ajev.1989.40.1.52

Naor, A., Gal, Y., & Bravdo, B. (2002). Shoot and Cluster Thinning Influence Vegetative Growth, Fruit Yield, and Wine Quality of `Sauvignon blanc' Grapevines. *J. Amer. Soc. Hortic. Sci*, *127*, 628–634. https://doi.org/10.21273/JASHS.127.4.628

Palliotti, A., & Cartechini, A. (2000). Cluster Thinning Effects on Yield and Grape Composition in Different Grapevine Cultivars. *Acta Hortic*, 111–120. https://doi.org/10.17660/ActaHortic.2000.512.11

Pereira, G. E., Padhi, E. M. T., Sudarshana, M. R., Fialho, F. B., Medina-Plaza, C., Girardello, R. C., Tseng, D., Bruce, R. C., Erdmann, J. N., Slupsky, C. M., & Oberholster, A. (2021). Impact of grapevine red blotch disease on primary and secondary metabolites in 'Cabernet-Sauvignon' grape tissues. *Food Chem*, *342*(128312). https://doi.org/10.1016/j.foodchem.2020.128312

Poojari, S., Alabi, O. J., Fofanov, V. Y., & Naidu, R. A. (2013). *A Leafhopper-Transmissible DNA Virus with Novel Evolutionary Lineage in the Family Geminiviridae Implicated in Grapevine Redleaf Disease by Next-Generation Sequencing*. https://doi.org/10.1371/journal.pone.0064194

Reynard, J.-S., Brodard, J., Dubuis, N., Zufferey, V., Schumpp, O., Schaerer, S., & Gugerli, P. (2018). Grapevine Red Blotch Virus: Absence in Swiss Vineyards and Analysis of Potential Detrimental Effect on Viticultural Performance. *Plant Dis*, *102*, 651–655. https://doi.org/10.1094/PDIS-07-17-1069-RE

Ricketts, K. D., Gómez, M. I., Fuchs, M. F., Martinson, T. E., Smith, R. J., Cooper, M. L., Moyer, M. M., & Wise, A. (2017). Mitigating the Economic Impact of Grapevine Red Blotch: Optimizing Disease Management Strategies in U.S. *Vineyards. Amer. J. Enol. Viticult*, *68*, 127–135. https://doi.org/10.5344/ajev.2016.16009

Rumbaugh, A. C., Girardello, R. C., Cooper, M. L., Plank, C., Kurtural, S. K., & Oberholster, A. (2021). Impact of Rootstock and Season on Red Blotch Disease Expression in Cabernet-Sauvignon (V. *vinifera*. *Plants*, *10*(1583). https://doi.org/10.3390/plants10081583

Sudarshana, M. R., Perry, K. L., & Fuchs, M. F. (2015). Grapevine Red Blotch-Associated Virus, an Emerging Threat to the Grapevine Industry. *Phytopathology*, *105*, 1026–1032. https://doi.org/10.1094/PHYTO-12-14-0369-FI

Swamy, P., Pattathil, S., Unda, F., & Mansfield, S. D. (2021). *Grapevine Red Blotch Disease Affects Carbohydrate Homeostasis and Cell Call Characteristics in Vitis Vinifera L*. https://doi.org/10.21203/rs.3.rs-428067/v1

Terry, D. B., & Kurtural, S. K. (2011). Achieving Vine Balance of Syrah with Mechanical Canopy Management and Regulated Deficit Irrigation. *Amer. J. Enol. Viticult*, *62*, 426–437. https://doi.org/10.5344/ajev.2011.11022

Torres, N., Martínez-Lüscher, J., Porte, E., & Kurtural, S. K. (2020). Optimal Ranges and Thresholds of Grape Berry Solar Radiation for Flavonoid Biosynthesis in Warm Climates. *Frontiers in Plant Science*, *11*(931). https://doi.org/10.3389/fpls.2020.00931

Torres, N., Martínez-Lüscher, J., Porte, E., Yu, R., & Kurtural, S. K. (2021). Impacts of Leaf Removal and Shoot Thinning on Cumulative Daily Light Intensity and Thermal Time and Their Cascading Effects of Grapevine (*Vitis vinifera* L.) Berry and Wine Chemistry in Warm Climates. *Food Chemistry*, *343*(128447). https://doi.org/10.1016/j.foodchem.2020.128447

Torres, N., Yu, R., Martínez-Lüscher, J., Kostaki, E., & Kurtural, S. K. (2021). Application of Fractions of Crop Evapotranspiration Affects Carbon Partitioning of Grapevine Differentially in a Hot Climate. *Frontiers in Plant Science*, *12*(75). https://doi.org/10.3389/fpls.2021.633600

Wallis, C. M., & Sudarshana, M. R. (2016). *Effects of Grapevine Red Blotch-Associated Virus*.

Yu, R., & Kurtural, S. K. (2020). *Proximal Sensing of soil electrical conductivity provides a link to Soil-Plant Water Relationships and Supports the Identification of Plant Water Status Zones in Vineyards*. https://doi.org/10.3389/fpls.2020.00244.